

Studying real-time properties of gauge theories

Kirill Boguslavski

Institute for Theoretical Physics
TU Wien, Austria

Theory Seminar,
Subatech, Nantes, January 01, 2024

Talk based on (selection):

Complex Langevin: KB, Hotzy, Müller, 2212.08602, 2312.03063

\hat{q} , κ : KB, Kurkela, Lappi, Lindenbauer, Peuron, 2303.12595, 2303.12520



TECHNISCHE
UNIVERSITÄT
WIEN



Der Wissenschaftsfonds.

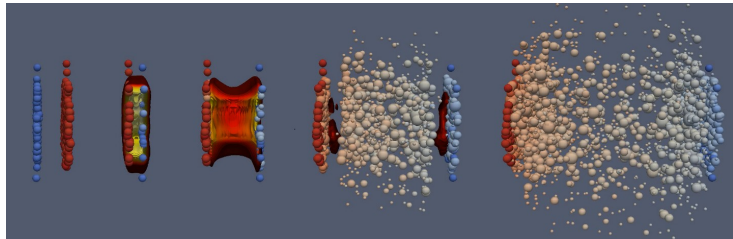
Table of Contents

- 1 Motivation
- 2 Spectral functions in the quark-gluon plasma
- 3 Transport coefficients
- 4 Towards simulations of real-time lattice gauge theory
- 5 Conclusion

Table of Contents

- 1 Motivation
- 2 Spectral functions in the quark-gluon plasma
- 3 Transport coefficients
- 4 Towards simulations of real-time lattice gauge theory
- 5 Conclusion

Stages in heavy-ion collisions



MADAI collaboration

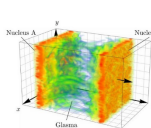
- High-energy collisions \Rightarrow **Quark-Gluon plasma (QGP)** created
- Cooling during evolution, go through different **phases**
 \Rightarrow pre-equilibrium QGP \rightarrow fluid QGP \rightarrow hadrons
- At early times, **pre-equilibrium QGP** phase (initial stages) involves large gluon fields $A \sim 1/g$, then quasiparticle excitations
 \Rightarrow classical-statistical simulations \Rightarrow QCD kinetic theory

Goal

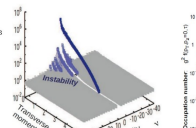
Learn about real-time properties of QCD

Initial stages in heavy-ion collisions (weak- g^2 perspective)

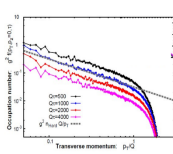
$$Q_s \tau = 0^+$$



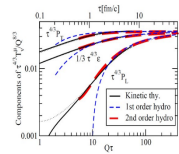
$$Q_s \tau = \ln^2(\alpha_s^{-1})$$



$$Q_s \tau = \alpha_s^{-3/2}$$



$$Q_s \tau = \alpha_s^{-13/5}$$



Glasma

Instabilities

Bottom-up stage 1

Bottom-up stages 2 and 3

Onset of hydrodynamics

$$D_\mu F^{\mu\nu} = J^\nu$$

classical-statistical simulations

$$-\frac{\partial f_{\vec{p}}}{\partial \tau} = \mathcal{C}^{1 \leftrightarrow 2}[f_{\vec{p}}] + \mathcal{C}^{2 \leftrightarrow 2}[f_{\vec{p}}] - \frac{p_z}{\tau} \frac{\partial f_{\vec{p}}}{\partial p_z}$$

QCD effective kinetic theory simulations

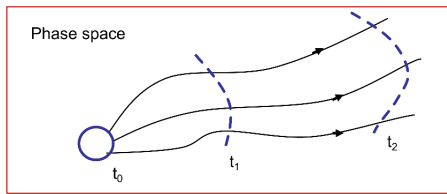
hydrodynamics ...

Table of Contents

- 1 Motivation
- 2 Spectral functions in the quark-gluon plasma
- 3 Transport coefficients
- 4 Towards simulations of real-time lattice gauge theory
- 5 Conclusion

Classical-statistical simulations

- At initial time t_0 set (quantum) **initial conditions** (IC):
⇒ Choose $\langle AA \rangle$, $\langle EE \rangle$ in x or p space
- Approximate quantum dynamics with **classical EOMs** $D_\mu F^{\mu\nu} = 0$
⇒ Gauge co-variant lattice formulation using links $U_j(x) = e^{ig a_j A_j(x)}$
- Obtain observables at t by **averaging** over trajectories (same IC)

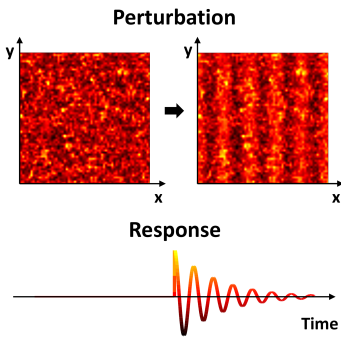


- Applicability limited to earliest times when $f(t, \vec{p}) \sim \langle EE \rangle / p \gg 1$
- Also kinetic theory, hydro, AdS/QCD are based on approximations

Quasiparticles? Extract gluon spectral function ρ

Classical-statistical $SU(N_c)$ simulations + linear response theory

KB, Kurkela, Lappi, Peuron, *PRD 98, 014006 (2018)*



- Similar algorithm for fermions
- Split $A(t, \vec{x}) \mapsto A(t, \vec{x}) + \delta A(t, \vec{x})$ at t , perturb with plane wave $j_0(\vec{p}) \delta(t' - t)$
- Response $\langle \delta A(t', \vec{p}) \rangle = G_R(t', t, \vec{p}) j_0(\vec{p})$
- Linearized EOM for $\delta A(t, \vec{x})$ such that Gauss law conserved (also in gauge-cov. formulation)

Kurkela, Lappi, Peuron, *EUJC 76 (2016) 688*

- $\theta(t' - t) \boxed{\rho(t', t, p)} = G_R(t', t, p)$
- Fourier transform $\rho(\bar{t}, \omega, p)$ ($\bar{t} = \frac{1}{2}(t + t')$)

Very similar methods for scalars:

Aarts (2001); Piñeiro Orioli, Berges (2019); Schlichting, Smith, von Smekal (2020); KB, Piñeiro Orioli (2020); ...

What excitations drive the dynamics in the QGP?

Study microscopics of the Quark-Gluon plasma

Quasiparticles? Fluct.-diss. relation (FDR)? When is kinetic theory valid?

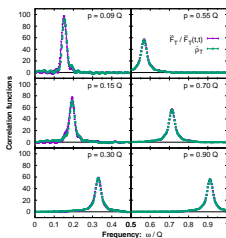
- Spectral function $\dot{\rho}(t, \omega, p) \sim \langle [\hat{A}, \hat{E}] \rangle$ encodes excitation spectrum!
- Statistical correlator $\ddot{F}(t, \omega, p) \sim \langle \{ \hat{E}, \hat{E} \} \rangle$ appears related

What excitations drive the dynamics in the QGP?

Study microscopics of the Quark-Gluon plasma

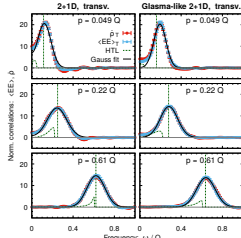
Quasiparticles? Fluct.-diss. relation (FDR)? When is kinetic theory valid?

- Spectral function $\rho(t, \omega, p) \sim \langle [\hat{A}, \hat{E}] \rangle$ encodes excitation spectrum!
- Statistical correlator $\ddot{F}(t, \omega, p) \sim \langle \{\hat{E}, \hat{E}\} \rangle$ appears related
⇒ generalized FDR: $\ddot{F}(t, \omega, p)/\ddot{F}(t, t, p) \approx \rho(t, \omega, p)$

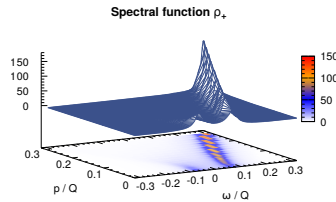


Gluonic 3+1D

KB, Kurkela, Lappi, Peuron, PRD 98 (2018) 014006;
PRD 100 (2019) 094022; JHEP 05 (2021) 225



Gluonic 2+1D



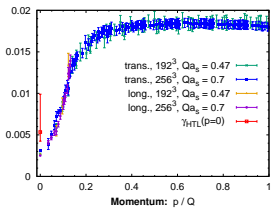
Fermionic 3+1D

KB, Lappi, Mace, Schlichting, PLB 827 (2022) 136963

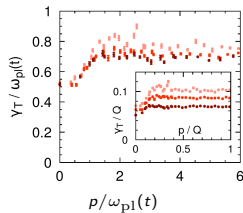
Spectral functions: width of excitations (inverse lifetimes)

Examples: First principles' determination of damping rates $\gamma(t, p)$ in isotropic highly-occupied QGP (as on a slide before)

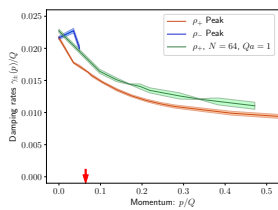
Gluonic 3+1D



Gluonic 2+1D



Fermionic 3+1D



$\gamma \ll \omega_{\text{pl}}$, increasing in p

$\gamma \sim \omega_{\text{pl}}$

$\gamma \ll \omega_{\text{pl}}$, decreasing in p

- ⇒ 3+1D: well described by perturbation theory (except fermions low p)
- ⇒ gluonic 2+1D: no quasiparticles for $p \lesssim \omega_{\text{pl}}$; Anisotropic kinetics?
- ⇒ HTL / kinetic theory in 2+1D may require nonperturbative IR

Table of Contents

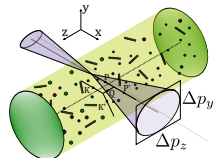
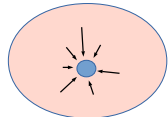
- 1 Motivation
- 2 Spectral functions in the quark-gluon plasma
- 3 Transport coefficients
- 4 Towards simulations of real-time lattice gauge theory
- 5 Conclusion

Transport coefficients κ, \hat{q} from pre-equilibrium QGP

Jets, heavy quarks: potential for signatures of initial stages
medium interactions \Rightarrow QGP properties encoded in observables

- Quarks/jets get 'kicks' $\dot{p}_i(\tau) = \mathcal{F}_i(\tau)$
- Heavy-quark diffusion coefficient $\kappa_i = \frac{d}{d\tau} \langle p_i^2 \rangle$
 \Rightarrow heavy quark has small momentum $p \ll M$
- κ enters Lindblad eq. for **quarkonium dynamics**
Brambilla, Escobedo, [Soto], [Strickland], Vairo, [v.d. Griend, Weber] (2016, 2021)
- Jet quenching parameter $\hat{q}_i = \frac{d}{d\tau} \langle p_{\perp,i}^2 \rangle$
 \Rightarrow jet with high momentum $p \gg Q_s, T$
- Pre-equilibrium **dynamics encoded** in heavy-quark diffusion, quarkonia and jet quenching

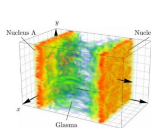
Mrowczynski (2018); Ruggieri, Das (2018); Sun, Coci, Das, Plumari, Ruggieri, Greco (2019); Ipp, Müller, Schuh (2020); KB, Kurkela, Lappi, Peuron (2020); Khowal, Das, Oliva, Ruggieri (2022); Carrington, Czajka, Mrowczynski (2020, 2022); Barata, Sadofyev, Wang (2023); Andres, Apolinário, Dominguez, Martinez, Salgado (2023); Avramescu, Baran, Greco, Ipp, Müller, Ruggieri (2023); KB, Kurkela, Lappi, Lindenbauer, Peuron (2023); Du (2023), ...



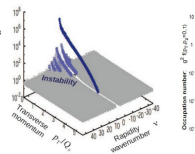
KB, Kurkela, Lappi, Lindenbauer, Peuron (2023)

Initial stages in heavy-ion collisions (weak- g^2)

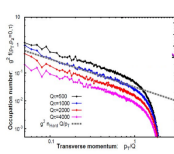
$$Q_s \tau = 0^+$$



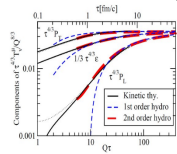
$$Q_s \tau = \ln^2(\alpha_s^{-1})$$



$$Q_s \tau = \alpha_s^{-3/2}$$



$$Q_s \tau = \alpha_s^{-13/5}$$



Glasma

Instabilities

Bottom-up
stage 1

Bottom-up stages
2 and 3

Onset of
hydrodynamics

$$D_\mu F^{\mu\nu} = J^\nu$$

classical-statistical simulations

$$-\frac{\partial f_{\vec{p}}}{\partial \tau} = \mathcal{C}^{1 \leftrightarrow 2}[f_{\vec{p}}] + \mathcal{C}^{2 \leftrightarrow 2}[f_{\vec{p}}] - \frac{p_z}{\tau} \frac{\partial f_{\vec{p}}}{\partial p_z}$$

QCD effective kinetic theory simulations

hydrodynamics ...

Heavy quark diffusion in a Glasma model

KB, Kurkela, Lappi, Peuron, JHEP 09, 077 (2020)

$$\langle p^2(t, \Delta t) \rangle = \frac{g^2}{2N_c} \int_t^{t+\Delta t} dt' \int_t^{t+\Delta t} dt'' \langle EE \rangle(t', t'')$$

$$\begin{aligned} 3\kappa(t, \Delta t) &= \frac{d}{d\Delta t} \langle p^2(t, \Delta t) \rangle \\ &\approx \frac{g^2}{N_c} \int_{-\infty}^{\infty} \frac{d\omega}{2\pi} \frac{\sin(\omega \Delta t)}{\omega} \langle EE \rangle(t, \omega) \end{aligned}$$

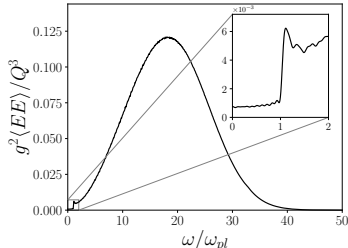
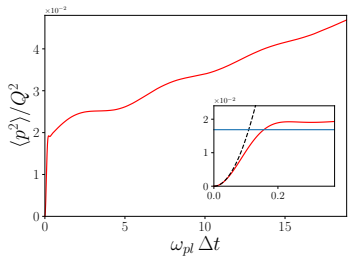
Three features \Rightarrow explained by $\langle EE \rangle$ or ρ

- ➊ quadratic initial growth
- ➋ oscillations from quasiparticles
- ➌ diffusion from Landau damping

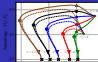
\Rightarrow Knowledge of correlators essential!

Also in the Glasma: large κ and $\kappa_z > \kappa_T$

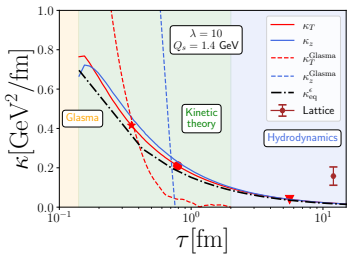
Ipp, Müller, Schuh (2020); Carrington, Czajka, Mrowczynski (2022); Khowal, Das, Oliva, Ruggieri (2022); Avramescu et al. (2023)



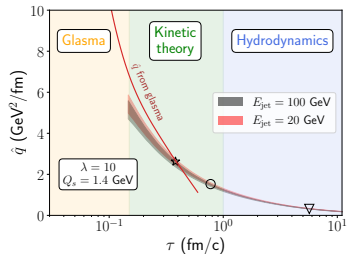
κ and \hat{q} during bottom-up (kinetic evolution)



κ of heavy quarks



\hat{q} of jets



KB, Kurkela, Lappi, Lindenbauer, Peuron; for κ [2303.12520], for \hat{q} [2303.12595], [2312.00447],

limiting attractors for κ & \hat{q} [2312.11252]

- Close gap in κ and \hat{q} between Glasma and hydro via **kinetic theory**
 - \hat{q} smoothly connects Glasma and hydro, little sensitivity to details
 - κ_i less smooth (esp. κ_z), estimate $\langle p^2 \rangle = \int d\tau 3\kappa(\tau) \sim 1 \text{ GeV}^2$
 - Mostly the same ordering $\kappa_z > \kappa_T$ and $\hat{q}_z > \hat{q}_y$
 - ⇒ Observable via jet **polarisation?** (Hauksson, Iancu (2023))
 - ⇒ Impact on **jet energy loss?**
 - ⇒ Pheno. impact of $\kappa_i(\tau)$ on **heavy quarks/quarkonia?**

Table of Contents

- 1 Motivation
- 2 Spectral functions in the quark-gluon plasma
- 3 Transport coefficients
- 4 Towards simulations of real-time lattice gauge theory
- 5 Conclusion

Complex Langevin: towards ab-initio framework for QCD

This section is based on:

KB, Hotzy, Müller, *JHEP 06, 011 (2023) [2212.08602]*

KB, Hotzy, Müller, *2312.03063*



P. Hotzy



D.I. Müller

- Spectral functions, transport coefficients, viscosities are based on **real-time correlations**
- Such observables difficult to compute in **Lattice QCD** (Euclidean)
- **No general ab-initio** pre-equilibrium framework for QCD exists
- Existing methods (classical-statistical, kinetic theory, hydrodynamics) have **limited applicability**

Can we develop an ab-initio pre-equilibrium framework for QCD?

NP-hard sign problem due to complex action!

Observables in the real-time formalism

- **Path integral expression** for expectation values:

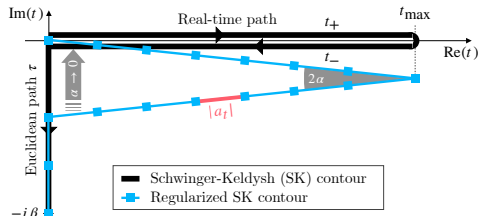
$$\langle \mathcal{O}[A] \rangle = \frac{1}{Z} \int \mathcal{D}A_E e^{-S_E[A_E]} \int \mathcal{D}A_+ \mathcal{D}A_- e^{iS[A_+, A_-]} \mathcal{O}[A_+, A_-, A_E]$$

- **Yang-Mills action:**

$$S_{\text{YM}} = -\frac{1}{4} \int_{\mathcal{C}_\pm, \mathcal{C}_E} d^4x F_a^{\mu\nu} F_a^{\mu\nu}$$

- **Correlation functions of $T^{\mu\nu}$:**

- speed of sound
- bulk- and shear-viscosity
- spectral functions



First: (Real) Langevin method

- **Langevin** method for Euclidean Yang-Mills theory

$$\partial_\theta A_\mu^a(\theta, x) = -\frac{\delta S_E}{\delta A_\mu^a(\theta, x)} + \eta_\mu^a(\theta, x),$$
$$\langle \eta \rangle = 0, \quad \langle \eta(\theta)\eta(\theta') \rangle \propto 2\delta(\theta - \theta').$$

- Equivalent to **Fokker-Planck equation** via Ito's Lemma

$$\partial_\theta P(A, \theta) = \delta_A (\delta_A + \delta_A S_E) P(A, \theta)$$

- Converges to **stationary** solution $P(A, \theta \rightarrow \infty) = \frac{1}{Z} \exp[-S_E[A]]$.

Expectation value by sampling at late θ

$$\langle \mathcal{O}[A] \rangle = \frac{1}{Z} \int \mathcal{D}A_E e^{-S_E[A_E]} \mathcal{O}[A(\theta)] \approx \lim_{\theta_0 \rightarrow \infty} \frac{1}{T} \int_{\theta_0}^{\theta_0+T} d\theta \mathcal{O}[A(\theta)]$$

Now: Complex Langevin for real-time Yang-Mills theory

- **Complex Langevin (CL)** method for Yang-Mills theory

$$\frac{\partial A_\mu^a(\theta, x)}{\partial \theta} = i \frac{\delta S_{\text{YM}}}{\delta A_\mu^a(\theta, x)} + \eta_\mu^a(\theta, x),$$

$$\langle \eta_\mu^a(\theta, x) \rangle = 0, \quad \langle \eta_\mu^a(\theta, x) \eta_\nu^b(\theta', y) \rangle = 2\delta(\theta - \theta')\delta^{(4)}(x - y)\delta^{ab}\delta_{\mu\nu}.$$

- **Complexification** of Lie algebra: $SU(N) \rightarrow SL(N, \mathbb{C})$
- If process converges correctly, $A_\mu^a(\theta \rightarrow \infty, x)$ is described by

$$\rho[A] = \mathcal{N} \exp [iS_{\text{YM}}[A]]$$

CL bypasses the sign problem by sampling at late θ

$$\langle \mathcal{O}[A] \rangle = \int \mathcal{D}A \rho[A] \mathcal{O}[A] \approx \lim_{\theta_0 \rightarrow \infty} \frac{1}{T} \int_{\theta_0}^{\theta_0 + T} d\theta \mathcal{O}[A(\theta)]$$

Complex Langevin on the lattice

- Link variables and plaquette variables

$$U_{x,\mu} \simeq \exp [ig a_\mu A_\mu(x + \hat{\mu}/2)] \in \mathrm{SU}(N_c) \rightsquigarrow \mathrm{SL}(N_c, \mathbb{C}),$$

$$U_{x,\mu\nu} = U_{x,\mu} U_{x+\hat{\mu},\nu} U_{x+\hat{\nu},\mu}^{-1} U_{x,\nu}^{-1}$$

- Wilson plaquette action: $S_W[U] = \frac{1}{2N_c} \sum_{x,\mu \neq \nu} \beta_{\mu\nu} \mathrm{Tr}[U_{x,\mu\nu} - 1]$
- Coupling constants: $\beta_{0i} = -\frac{2N_c}{g^2} \frac{a_s}{a_{t,k}}, \quad \beta_{ij} = +\frac{2N_c}{g^2} \frac{\bar{a}_{t,k}}{a_s}$
- Averaged lattice spacing (time reversability): $\bar{a}_{t,k} = (a_{t,k} + a_{t,k+1})/2$

Update step for link variables

$$U_{x,\mu}(\theta + \epsilon) = \exp \left[it^a \left(i \Gamma_\mu \epsilon D_{x,\mu}^a S_W + \sqrt{\Gamma_\mu \epsilon} \eta_{x,\mu}^a(\theta) \right) \right] U_{x,\mu}(\theta)$$

⇒ Field independent kernel function Γ_μ leaves stationary solution intact
but can be utilised to **improve convergence and stability!**

New anisotropic kernel

- CL suffers from two types of **instabilities**: (Aarts, James, Seiler, Stamatescu (2011))
 - *Runaways*: numerical blowup of the solution
 - *Wrong convergence*: wrong results (assumptions violated)
- Several methods introduced to mitigate these issues (Backup): adaptive step size, gauge cooling, dynamical stabilization, *kernels*, ...

Anisotropic kernel

- We introduce an anisotropic kernel to alleviate instabilities
- $$\Gamma_t = |a_t|^2/a_s^2, \quad \Gamma_s = 1$$
- *Motivation*: Based on a careful rederivation of the CL equation on complex time contours. (Backup)
 - Previous studies used $\Gamma_\mu = 1$ (Berges, Borsanyi, Sexty, Stamatescu (2007))

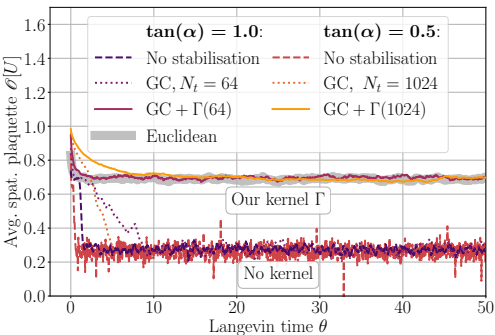
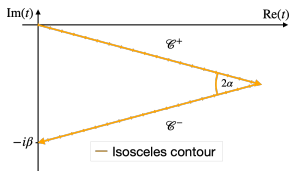
Stabilization (correct convergence) using Γ

Lattice parameters:
 $L = N_t \times 4^3$
 $g = 1, \beta = 1/T = 4$

- Reproduce SU(2) results of

(Berges, Borsanyi, Sexty, Stamatescu (2007))

- for $\mathcal{O}[U] = \frac{1}{6N_c N_x} \sum_{x,i \neq j} \text{Tr} [U_{x,ij}]$
- on isosceles contours



- Thermal (Euclidean)
 t -independent \rightarrow compare

- We find **metastable θ -region**

☒ Not-stabilised simulation:
Quickly wrong convergence

✓ Stabilised simulation:
Our kernel with GC reproduce
Euclidean results. ($N_t |a_t|$ fixed)

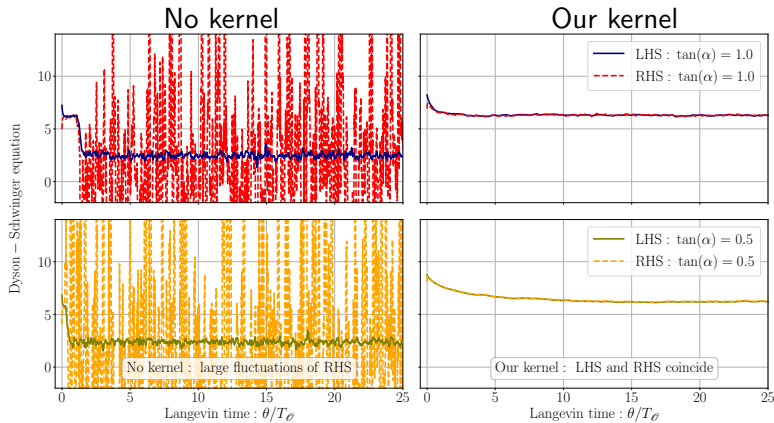
\Rightarrow Existing methods insufficient, our kernel stabilizes!

Dyson-Schwinger equations as probe for stability

- Self-consistency check of link configuration

$$\frac{2(N_c^2 - 1)}{N_c} \langle \text{ReTr}(U_{x,ij}) \rangle = \frac{i}{2N_c} \sum_{|\rho| \neq i} \beta_{i\rho} \left\langle \text{ReTr} \left[(U_{x,i\rho} - U_{x,i\rho}^{-1}) U_{x,ij} \right] \right\rangle$$

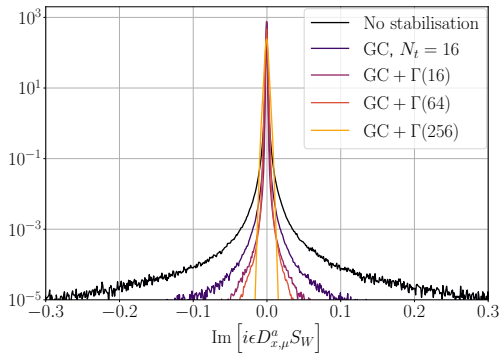
- RHS is very sensitive → probe for stability



Localized histogram of the drift terms

- Localised histograms of $\text{Im} [iDS_W]$ indicate **correct convergence**
- **No skirts/tails** using our kernel with sufficiently large N_t
- **Systematic improvement** using finer lattices (larger N_t)

- Gauge cooling helps, but skirts are still present
- Increasing N_t without our kernel does *not* improve the stability



Our simulation approach for real-time Yang Mills theory

- SK-contour needs regularization

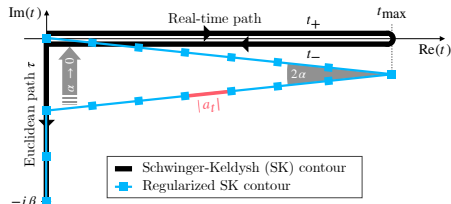
⇒ we **tilt the SK-contour**

⇒ instabilities more severe for smaller tilt angles

- Kernel alleviates instabilities

- **Metastability:** Region of correct convergence metastable. Increasing N_t systematically improves life time.

- **Observables** $\langle O \rangle$ calculated by averag. over region, then $\alpha \rightarrow 0$



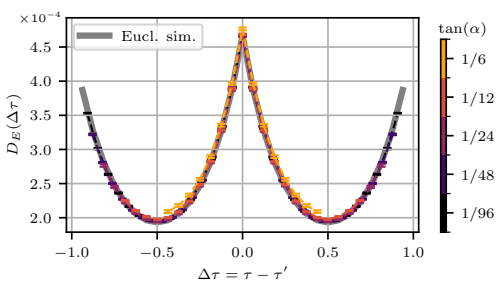
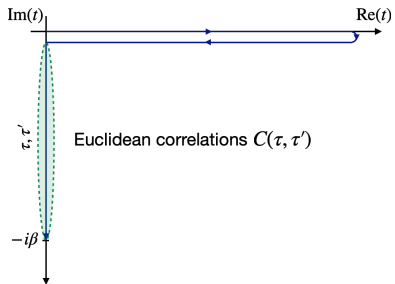
Unequal-time correlator (of B^2 , clover leaf) **for first time:**

$$C(t, t') = \frac{1}{N_s^3} \sum_x \langle B^2(t, x) B^2(t', x) \rangle - \langle B^2 \rangle^2$$

Euclidean correlation function

Lattice parameters:
 $L = 64 \times 16^3$
 $g = 0.5, \beta = 1/T = 1$

- Euclidean correlation function $C(\tau, \tau')$ along thermal path
- Coinciding with correlation function from Euclidean simulation
⇒ **Independence** of tilt angle α

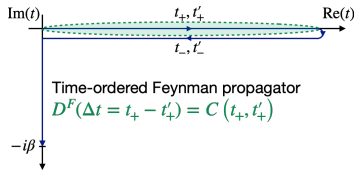


Limit towards Schwinger-Keldysh-contour $\alpha \rightarrow 0$

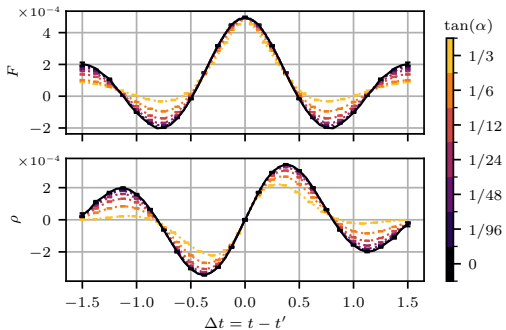
Statistical & spectral functions

- Decreasing tilt angle leads to “converging” Feynman propagator D^F .

⇒ **Justification** for extrapolation $\alpha \rightarrow 0$.



$$\begin{aligned} F &= \text{Re } D^F \\ \rho &= -\text{sgn}(\Delta t) \text{Im } D^F \end{aligned}$$

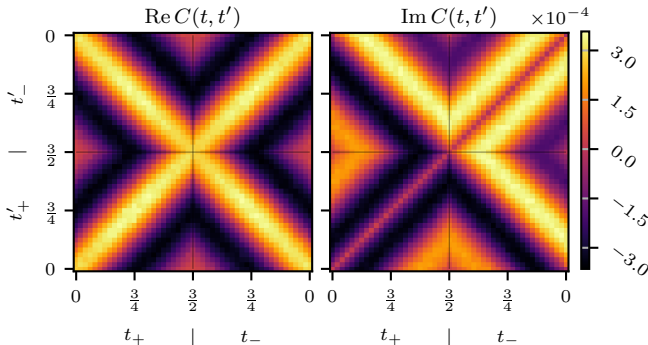


Extrapolated to the Schwinger-Keldysh contour

- **Real-time correlations** for SU(2) Yang-Mills theory in 3+1D
- Quadrants correspond to different propagators (Feynamn, Wightman)

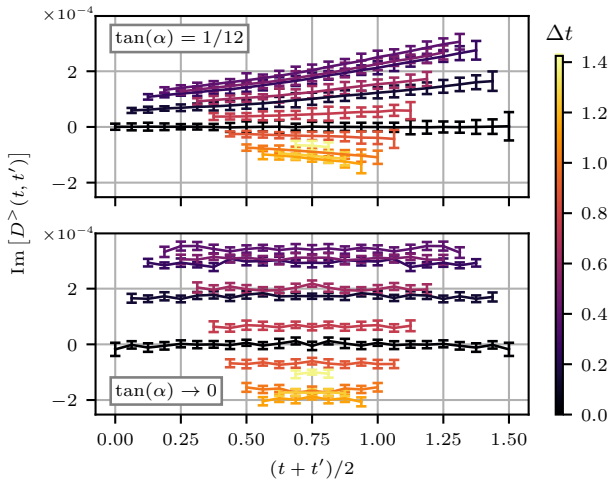
$$D^<(t, t') = C(t_+, t'_-) \quad D^{\bar{F}}(t, t') = C(t_-, t'_-)$$

$$D^F(t, t') = C(t_+, t'_+) \quad D^>(t, t') = C(t_-, t'_+)$$



Emergent time translation invariance for $\alpha \rightarrow 0$

- Thermal equilibrium: correlations independent of $(t + t')/2$
- Independence found numerically only in limit $\alpha \rightarrow 0$



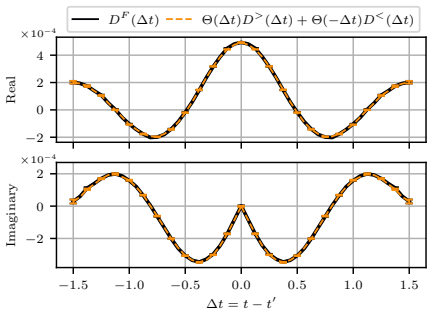
Consistency among propagators only for $\alpha \rightarrow 0$

- Feynman propagator and Weightman functions **analytically related**

$$D^F(t - t') = \theta(t - t') D^>(t, t') + \theta(t' - t) D^<(t, t')$$

- Relation established only in the limit $\alpha \rightarrow 0$

Limit $\alpha \rightarrow 0$



$\alpha \rightarrow 0$ vs. finite α

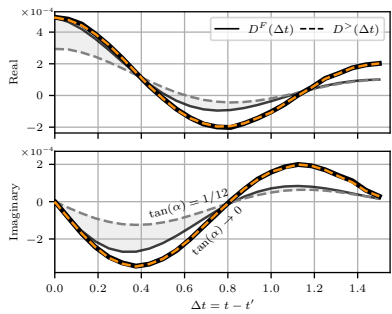


Table of Contents

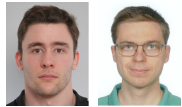
- 1 Motivation
- 2 Spectral functions in the quark-gluon plasma
- 3 Transport coefficients
- 4 Towards simulations of real-time lattice gauge theory
- 5 Conclusion

Research group

- ★ *Postdoc:*
David Müller



- ★ *PhDs:*
Paul Hotzy, Florian Lindenbauer



- ★ *Master thesis, Master project:*
Alois Altenburger, Tobias Angelli, Liane Backfried,
Fabian Helmberger



Conclusion

- Initial stages of the QGP \Rightarrow class.-stat., kinetics, hydro
- Spectral functions, unequal-time correlators
 - \Rightarrow Reveal excitations, explain medium properties
 - \Rightarrow Nonperturbative computation in pre-equilibrium QGP
- Transport coefficients κ, \hat{q}
 - \Rightarrow encode dynamics of QGP
 - \Rightarrow different features, anisotropic $\kappa_z > \kappa_T, \hat{q}$ smooth transition
- Complex Langevin (CL) \Rightarrow towards direct real-time simulations
 - \Rightarrow First direct calculation of (t, t') correlators (3+1D lattice SU(2))

Outlook

- Impact of medium $\kappa_i(\tau), \hat{q}_i(\tau)$ on heavy quarks, quarkonia, jets?
- CL method currently limited \Rightarrow larger g, t_{\max} ? renormalization?
- Application of SU(N) out of equilibrium?

Thank you for your attention!

Backup slides

Gluon ρ

Gluon unequal-time correlations

in 3+1D:

KB, Kurkela, Lappi, Peuron, *PRD 98, 014006 (2018) [1804.01966]*

in 2+1D:

KB, Kurkela, Lappi, Peuron, *JHEP 05, 225 (2021) [2101.02715]*

- Spectral function ($\dot{\rho} = \partial_t \rho$, $E = \partial_t A$)

$$\rho(x', x) = \frac{i}{N_c^2 - 1} \left\langle \left[\hat{A}(x'), \hat{A}(x) \right] \right\rangle$$

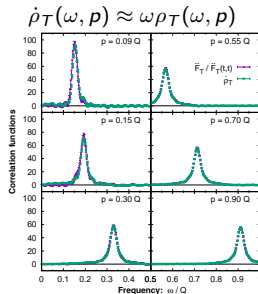
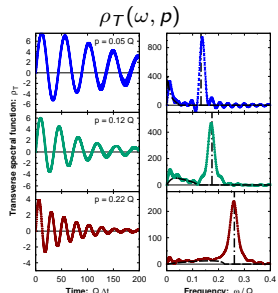
- Statistical correlator $\langle EE \rangle$ ($\equiv \ddot{F}$), in general independent of $\dot{\rho}$

$$\langle EE \rangle(x', x) = \frac{1}{2(N_c^2 - 1)} \left\langle \left\{ \hat{E}(x'), \hat{E}(x) \right\} \right\rangle$$

- Classical-statistical: $\langle EE \rangle(t', t, p) = \frac{1}{N_c^2 - 1} \langle E(t', \vec{p}) E^*(t, \vec{p}) \rangle$

Gluon ρ in 3+1D: compare with HTL perturbation theory

KB, Kurkela, Lappi, Peuron, PRD 98, 014006 (2018)



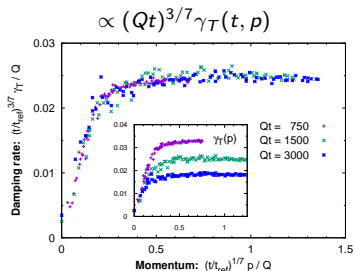
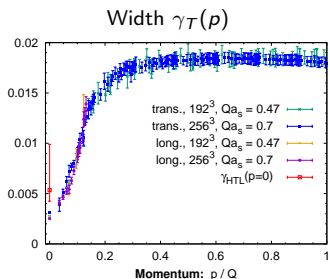
- **Narrow Lorentzian q.p. peaks** (position $\omega(p)$, width $\gamma(p)$)
- **HTL at LO (black dashed)** describes main features well
- Landau cut ($\omega < p$) and q.p. peak **distinguishable**
- Generalized fluctuation dissipation relation (**FDR**)

$$\frac{\langle EE \rangle_\alpha(t, \omega, p)}{\langle EE \rangle_\alpha(t, \Delta t=0, p)} \approx \frac{\dot{\rho}_\alpha(t, \omega, p)}{\dot{\rho}_\alpha(t, \Delta t=0, p)}$$

$\ddot{F} \equiv \langle EE \rangle$, $\alpha = T, L$ polarizations

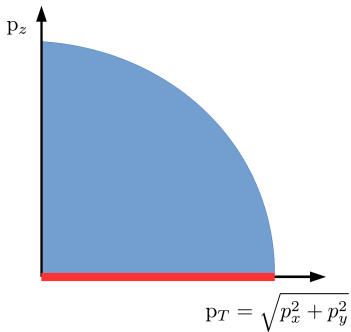
Gluon ρ in 3+1D: Damping rates (quasiparticle width)

KB, Kurkela, Lappi, Peuron, PRD 98, 014006 (2018)



- Peak width $\gamma(t, p) \ll \omega(t, p)$ beyond HTL at LO
- $\gamma_T(t, p)$ increases with p (different from fermion $\gamma_+(t, p)$)
(vs. HTL prediction $\gamma(p=0)$, $\gamma(p \rightarrow \infty)$, Braaten, Pisarski (1990); Pisarski (1992))
- Self-similar scaling $\Rightarrow \frac{\gamma_\alpha(t, p)}{\omega(t, p=0)} \sim (Qt)^{-2/7}$ decreases as expected
(different from fermions where $\frac{\gamma_+(t, p=0)}{\omega_+(t, p=0)} \approx \text{const}$)

Systems in 3+1D \rightarrow 2+1D

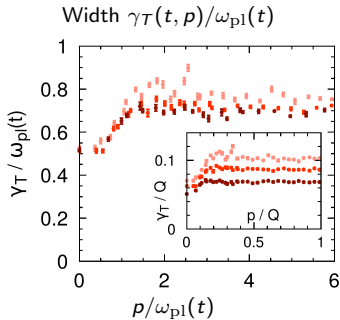
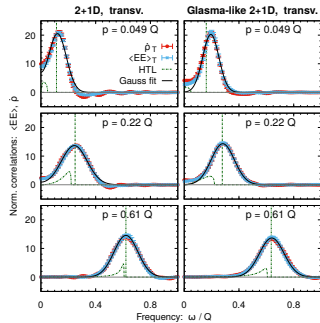


- Isotropic 3+1D: $f(t, p)$
- 2+1D: $f(t, p_T, p_z=0)$
- can be regarded as extreme momentum anisotropy

Gluon ρ in 2+1D

KB, Kurkela, Lappi, Peuron, JHEP 05, 225 (2021)

$$\dot{\rho}_T(\omega, p) \approx \omega \rho_T(\omega, p)$$



- ✓ Generalized FDR, but:
- ✗ Broad non-Lorentzian peaks
- ✗ HTL curves (green) agree poorly
- ✗ Landau cut and q.p. peak not distinguishable

- Peak width $\gamma_T(t, p) \sim \omega_{\text{pl}}(t)$
($\omega_{\text{pl}} \equiv \omega_T(p=0)$)

⇒ no quasiparticles for $p \lesssim \omega_{\text{pl}}$!

Fermion ρ

Fermion spectral function

KB, Lappi, Mace, Schlichting, *PLB 827, 136963 (2022) [2106.11319]*

- $SU(N_c)$ gauge theory (simulations: $N_c = 2$, $U_j \approx \exp(ig a_s A_j)$)

$$H_{YM} = \frac{1}{g^2 a_s} \sum_{\vec{x}, i} \text{Tr}[E_i(t', \vec{x})^2] + \frac{1}{2} \sum_j \text{ReTr}[1 - U_{ij}(t', \vec{x})]$$
$$\hat{H}_W = \frac{1}{2} \sum_{\vec{x}} [\hat{\psi}^\dagger(t', \vec{x}), \gamma^0 (-i \not{D}_s[U] + m) \hat{\psi}(t', \vec{x})]$$

- Neglect fermionic backreaction (suppressed), temporal gauge $A_0 = 0$, mode expansion, plane waves at reference time t

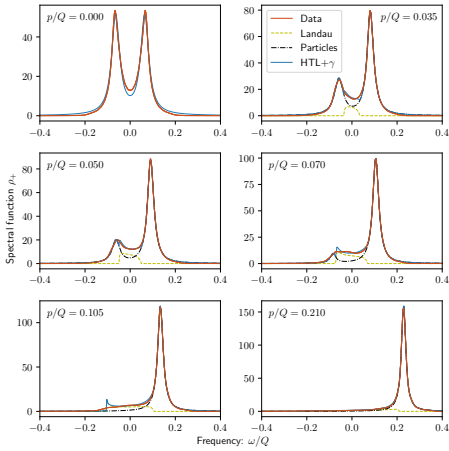
See also: Aarts, Smit (1999); Kasper, Hebenstreit, Berges (2014); Mace, Mueller, Schlichting, Sharma (2016); ...

- Definition $\rho^{\alpha\beta}(x', x) = \left\langle \left\{ \hat{\psi}^\alpha(t', \vec{x}'), \hat{\bar{\psi}}^\beta(t, \vec{x}) \right\} \right\rangle$
⇒ Fourier transform $\rho^{\alpha\beta}(t, \omega, p)$ via $t' - t$ and $\vec{x}' - \vec{x}$

Fermion ρ in 3+1D: Comparison with HTL

$$\rho_+(t, \omega, p) \equiv \rho_V^0 + \rho_V$$

$$(\rho_V^0 = \frac{1}{4} \text{Tr}(\rho \gamma^0), \rho_V = -\frac{E_p p^j}{4 p^2} \text{Tr}(\rho \gamma^j))$$



- **HTL+ γ extension**
(Landau cut + Lorentzian q.p. peaks:)

Braaten, Pisarski (1992); Rebhan (1992); Mrowczynski, Thomas (2000); Blaizot, Iancu (2002); ...

$$\begin{aligned} \rho_+^{\text{HTL}}(\omega, p) = & 2\pi \beta_+(\omega/p, p) \\ & + \frac{2Z_+(p)\gamma_+(p)}{(\omega - \omega_+(p))^2 + \gamma_+^2(p)} \\ & + \frac{2Z_-(p)\gamma_-(p)}{(\omega + \omega_-(p))^2 + \gamma_-^2(p)} \end{aligned}$$

- HTL dispersions $\omega_{\pm}(p)$ and residues $Z_{\pm}(p)$ agree with data

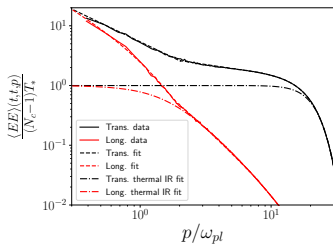
- Lattice 256^3 , $Qa_s = 0.75$, $m = 0.003125 Q$, $Qt = 1500$

Deep infrared and transport

Deep infrared (IR) of 3+1D gluonic plasmas

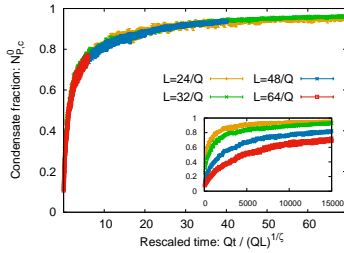
Can we understand the infrared ($p \ll Q$) of the pre-equilibrium QGP?

Excess of IR modes in $\langle EE \rangle$
correlators for $p \lesssim \omega_{pl}$



KB, Kurkela, Lappi, Peuron, JHEP 09 (2020) 077

Gauge-invariant condensation via
spatial Wilson and Polyakov loops



Berges, KB, Mace, Pawłowski, PRD 102 (2020) 034014

Berges, KB, Butler, de Bruin, Pawłowski, 2307.13669

- Excess of IR: observable in gauge-invariant κ (see below)
- Gauge-inv. cond. similar to Bose cond. in scalars \Rightarrow connection?

Far-from-equ. condensation in scalars: Berges, Sexty (2012); Piñero Orioli, KB, Berges (2015)

How to observe properties of the pre-equilibrium QGP?

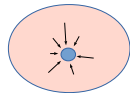
E.g., via impact on transport coefficients

As an example here, IR excess of gluons affects κ evolution

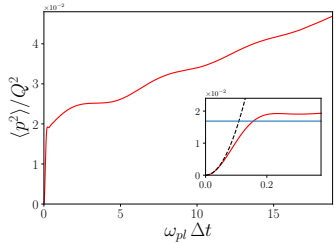
KB, Kurkela, Lappi, Peuron, *JHEP 09, 077 (2020)*

- Heavy quarks ‘kicked’ by the QGP medium

$$\dot{p}_i(t) = \mathcal{F}_i(t)$$



Momentum broadening

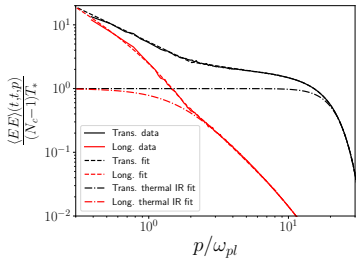


- Heavy-quark diffusion coefficient
 $3\kappa(t, \Delta t) = \frac{d}{d\Delta t} \langle p^2(t, \Delta t) \rangle$
- κ for bottomonium suppression
Brambilla, Escobedo, Soto, Vairo (2016)
- Impact on κ from IR excess

Approach: reconstruct κ using correlators $\dot{\rho}$ and $\langle EE \rangle$

$$3\kappa(t, \Delta t) \approx \frac{g^2}{N_c} \int \frac{d^3 p}{(2\pi)^3} \int_{-\infty}^{\infty} \frac{d\omega}{2\pi} \frac{\sin(\omega \Delta t)}{\omega} \\ \times \left[2\langle EE \rangle_T(t, t, p) \frac{\dot{\rho}_T(t, \omega, p)}{\dot{\rho}_T(t, t, p)} + \langle EE \rangle_L(t, t, p) \frac{\dot{\rho}_L(t, \omega, p)}{\dot{\rho}_L(t, t, p)} \right]$$

- use extracted equal-time and spectral functions in computation
- use $\langle EE \rangle_{T/L}(t, t, p)$ with IR excess ('data') & without ('thermal HTL')
- in $\dot{\rho}_{T/L}(t, \omega, p)$ Landau ($\omega < p$) and q.p. terms can be distinguished

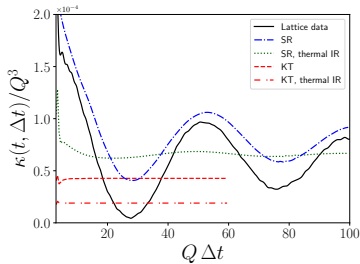


Gauge-invariant observation of IR gluon excess in κ

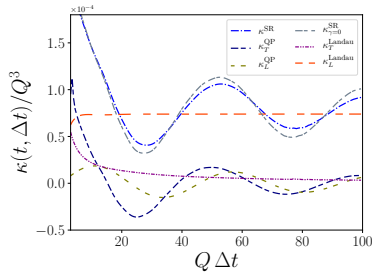
KB, Kurkela, Lappi, Peuron, JHEP 09 (2020) 077

$$\begin{aligned} \kappa(t, \Delta t) \approx & \frac{g^2}{3N_c} \int \frac{d^3 p}{(2\pi)^3} \int_{-\infty}^{\infty} \frac{d\omega}{2\pi} \frac{\sin(\omega \Delta t)}{\omega} \\ & \times \left[2\langle EE \rangle_T(t, t, p) \frac{\dot{\rho}_T(t, \omega, p)}{\dot{\rho}_T(t, t, p)} + \langle EE \rangle_L(t, t, p) \frac{\dot{\rho}_L(t, \omega, p)}{\dot{\rho}_L(t, t, p)} \right] \end{aligned}$$

Total $\kappa(t, \Delta t) \equiv \sum_i \kappa_i(t, \Delta t)$



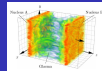
Components $\kappa_i(t, \Delta t)$



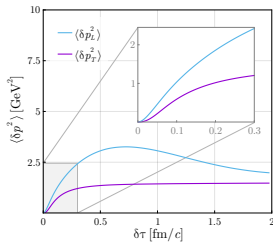
- Nonperturbative effects of $\langle EE \rangle_\alpha(t, t, p)$ and $\dot{\rho}_\alpha(t, \omega, p)$ visible!
- Oscillations with ω_{pl} due to QP excitations, sign of IR excess
- Heavy quarks, quarkonia, jets encode nonthermal dynamics of QGP

κ during initial stages

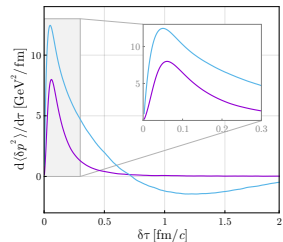
κ during Glasma phase



$\langle p_i^2 \rangle$ of beauty quarks

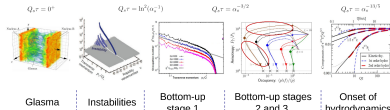


κ_i of beauty quarks



Avramescu, Baran, Greco, Ipp, Müller, Ruggieri PRD 107, 114021 (2023); 2307.07999

- Classical-statistical simulations of hard probes in the Glasma
 - Extraction of κ_i and \hat{q}_i in Glasma phase
Ipp, Müller, Schuh (2020); KB, Kurkela, Lappi, Peuron (2020); Carrington, Czajka, Mrowczynski (2022); Khowal, Das, Oliva, Ruggieri (2022); Avramescu et al. (2023)
 - Large values, anisotropic coefficients $\kappa_z > \kappa_T$ (z is beam direction)
- What about kinetic regime?



Kinetic theory \Rightarrow Bottom-up thermalization scenario

- **Bottom-up scenario**

Baier, Mueller, Schiff, Son, PLB (2001)

- Consists of **three stages**

- ➊ Classical attractor
- ➋ Anisotropy freezes
- ➌ Radiational breakup

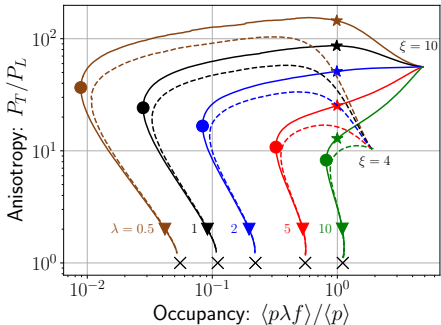
- Different bottom-up stages separated by markers ($\lambda = g^2 N_c$)

★ large pressure anisotropy

$$P_T \gg P_L, \text{ occupancy } f \sim 1/\lambda$$

● minimum (mean) occupancy f

▽ close to isotropic $P_T/P_L = 2$



Kurkela, Zhu (2015); version from:
KB, Kurkela, Lappi, Lindenbauer, Peuron (2023)

- Pressure $P_{T,L} \sim \int d^3 p \frac{p_{\perp,z}^2}{p} f$
- Mean $\langle O \rangle = \int d^3 p f(p) O(p)$

- Thermalization time scale $\tau_{\text{BMSS}} = \alpha_s^{-13/5} / Q_s$, initial momentum Q_s

QGP description: effective kinetic theory (EKT)

- When quasiparticles have formed: Kinetic theory applicable

Note: Assumes narrow excitations in spectral functions, which may not be true at low momenta for strong anisotropy (Backup in ' ρ ': 'Gluonic 2+1D')

KB, Kurkela, Lappi, Peuron (2018, 2019, 2021)

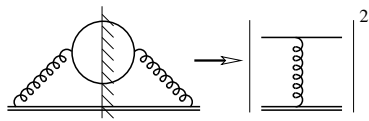
- Time evolution described by Boltzmann equation at LO

$$(\partial_t + \mathbf{v} \cdot \nabla) f = \left| \text{Y-shaped diagram with red lines} \right|^2 + \left| \text{Blue rectangle with red lines} \right|^2$$

$$\frac{\partial f_{\vec{p}}}{\partial \tau} - \frac{p_z}{\tau} \frac{\partial f_{\vec{p}}}{\partial p_z} = -\mathcal{C}^{2 \leftrightarrow 2}[f_{\vec{p}}] - \mathcal{C}^{1 \leftrightarrow 2}[f_{\vec{p}}]$$

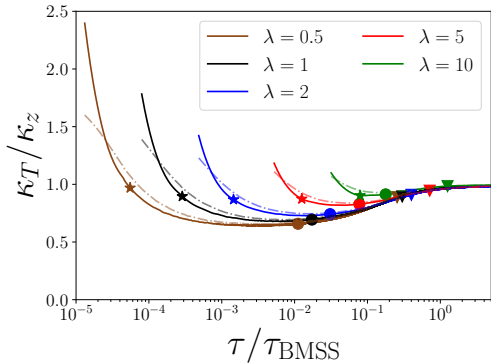
Arnold, Moore, Yaffe, JHEP 01, 030 (2003)

- Heavy-quark coefficient κ_i : Moore, Teaney (2005); Caron-Huot, Moore (2008)



Transverse vs. longitudinal diffusion

KB, Kurkela, Lappi, Lindenbauer, Peuron, 2303.12520



- $\kappa_T > \kappa_z$ during **over-occupied** stage (z is longitudinal/beam axis)
- $\kappa_T < \kappa_z$ after \star due to momentum anisotropy and **low occupancy**
- Most of the time $\kappa_T < \kappa_z$, anisotropy larger at weak coupling

Complex Langevin

Parametrization of the complex time contour

Unambiguous CL formalism

Introduce curve parameter λ for $t(\lambda)$ leads to

$$\partial_\theta A_\mu^a(\theta, \lambda, \vec{x}) = i \left. \frac{\delta S_{\text{YM}}}{\delta A_\mu^a(\lambda, \vec{x})} \right|_{A=A(\theta)} + \eta_\mu^a(\theta, \lambda, \vec{x}),$$

$$\langle \eta_\mu^a(\theta, \lambda, \vec{x}) \eta_\nu^b(\theta', \lambda', \vec{x}') \rangle = 2\delta_{\mu\nu}\delta^{ab}\delta(\theta - \theta')\delta(\lambda - \lambda')\delta^{(3)}(\vec{x} - \vec{x}')$$

- Complex time contours leads to **ambiguous noise correlator** expression (δ -distribution for complex arguments)
 - Ambiguities are resolved by a **path parameter** CL formulation

$$t : [a, b] \mapsto \mathbb{C}, \quad t(a) = 0, \quad t(b) = -i\beta$$

- Noise correlator in terms of λ

$$\delta(t(\lambda) - t(\lambda')) \rightsquigarrow \delta(\lambda - \lambda')$$

- Solution **independent** of chosen parametrization (kernel freedom)

Euler-Maruyama for numerical solution of the CLE

- Jacobian of parametrization leads to additional factors
- Lattice spacing a_λ of parametrization for contour

$$U_{x,t}(\theta + \epsilon) = \exp \left(it^a \left[i\epsilon \frac{a_\lambda}{a_s} \frac{\delta S_W}{\delta \tilde{A}_{x,t}^a} \Big|_\theta + \sqrt{\epsilon} \sqrt{\frac{a_\lambda}{a_s}} \eta_{x,\lambda}^a(\theta) \right] \right) U_{x,t}(\theta)$$

$$U_{x,i}(\theta + \epsilon) = \exp \left(it^a \left[i\epsilon \frac{a_s}{\bar{a}_\lambda} \frac{\delta S_W}{\delta \tilde{A}_{x,i}^a} \Big|_\theta + \sqrt{\epsilon} \sqrt{\frac{a_s}{\bar{a}_\lambda}} \eta_{x,i}^a(\theta) \right] \right) U_{x,i}(\theta)$$

CL update step for link variables on a SK-contour

- New update resolves ambiguities of complex time contour
- But introduces a divergence for $a_\lambda \rightarrow 0$
- Solution: rescale ϵ by a_s/a_λ or a_s/\bar{a}_λ (kernel freedom)

Existing CL stabilization techniques

- **Gauge cooling (GC):** Exploit gauge freedom to minimize non-unitarity measured by a functional $F[U]$ Seiler, Sexty, Stamatescu (2013)

$$U_{x,\mu} \mapsto U_{x,\mu}^V = V_x U_{x,\mu} V_{x+\mu}^{-1}, \quad F[U] \geq F[U^V]$$

- **Adaptive stepsize (AS):** Regulate large drift terms $K_{x,\mu}^a \equiv \frac{\delta S_W}{\delta \tilde{A}_{x,\mu}^a}$ which lead to instabilities (Aarts, James, Seiler, Stamatescu (2010))

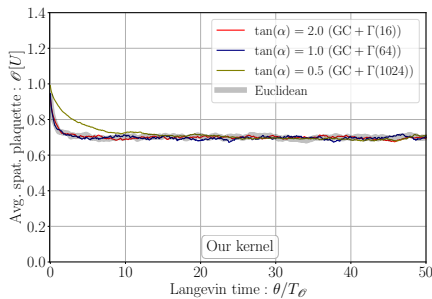
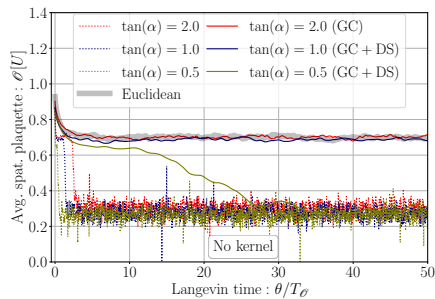
$$\epsilon \mapsto \tilde{\epsilon} = \epsilon \min \left(1, \frac{B}{\max_{x,\mu,a} |K_{x,\mu}^a|} \right)$$

- **Dynamical stabilization (DS):** Penalize drift terms depending on the local non-unitary of the configuration Attanasio, Jäger (2019)

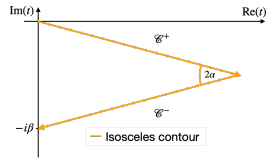
$$K_{x,\mu}^a \mapsto \tilde{K}_{x,\mu}^a = K_{x,\mu}^a + i\alpha_{DS} M_x^a,$$

$$M_x^a = b_x^a \left(\sum_c b_x^c b_x^c \right), \quad b_x^a = \sum_\mu \text{Tr}[t^a U_{x,\mu} U_{x,\mu}^\dagger]$$

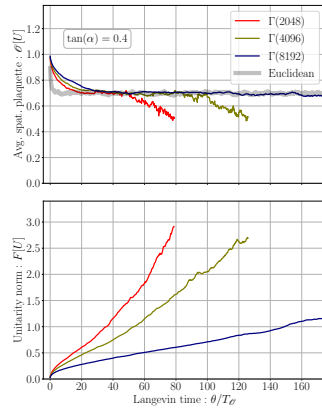
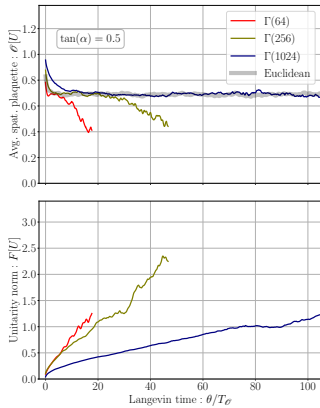
Anisotropic kernel comparison I



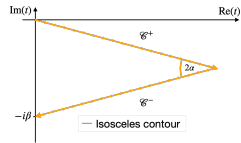
- Simulations on isosceles (see main part of the talk)
- Stabilization methods used:
 - GC: Gauge cooling
 - AS: Adaptive step size (everywhere)
 - DS: Dynamical stabilization



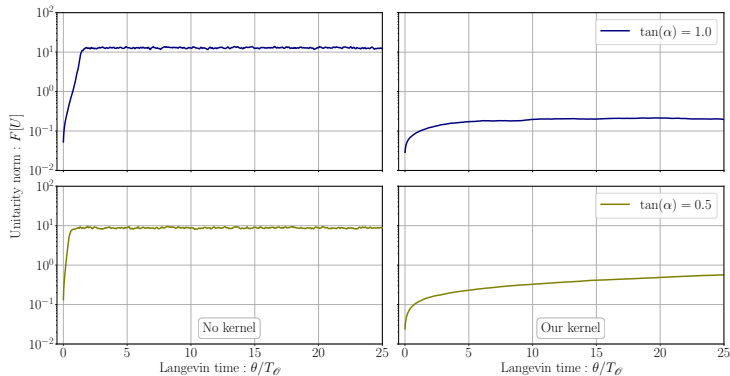
Anisotropic kernel comparison II



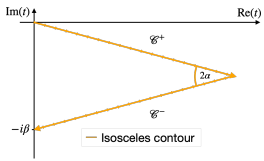
- Simulations on isosceles
- Systematic improvement on finer discretizations



Anisotropic kernel comparison III



- Simulations on isosceles
- $F[U] = \frac{1}{4N_t N_s^3} \sum_{x,\mu} \text{Tr} \left[(U_{x,\mu} U_{x,\mu}^\dagger - 1)^2 \right] \geq 0$
- Measure of how 'non-unitary' links are



Unitarity norm for unequal-time correlator simulations

- For different tilt angles of regularized SK contour
- Gray band indicates measurement region

